Available online at www.eccomasproceedia.org
Eccomas Proceedia SMART (2023) 1962-1973

ECCOMAS
Proceedia

X ECCOMAS Thematic Conference on Smart Structures and Materials
SMART 2023
D.A. Saravanos, A. Benjeddou, N. Chrysochoidis and T. Theodosiou (Eds)

NONLINEAR MODELING OF FERROELECTRIC PLATES AS ELECTRO-ELASTIC MATERIAL SURFACES

MICHAEL KROMMER* AND ASTRID PECHSTEIN*

*Institute of Technical Mechanics, Johannes Kepler University Linz
Altenbergerstraße 69, 4040 Linz, Austria
e-mail: {michael.krommer,astrid.pechstein}@jku.at
web page: http://www.jku.at/en/institute-of-technical-mechanics-tmech/

Abstract. We discuss nonlinear modeling of ferroelectric plates as electro-elastic material surfaces assuming the plate as a two-dimensional continuum with five mechanical degrees of freedom for each material point. Constitutive coupling by means of electrostriction, ferroelectric hysteresis and piezoelectricity are accounted for. For that sake, the augmented free energy is additively decomposed into an elastic part, a dielectric part and an augmentation energy. The elastic part involves an additive decomposition of the plate strain measures into elastic and electrical parts. Here, the electrical parts account for electrostriction and piezoelectricity, where electrostriction is assumed to depend quadratically on the polarization. For the dielectric part, we introduce the internal energy as a function of the polarization and an internal polarization, which allows us to accurately capture nonlinearities, such as saturation. Then, we compute the free energy applying a Legendre transformation, such that the voltage enters the formulation. The augmentation energy accounts for the contribution from vacuum. Finally, we introduce a so-called dissipation function, by means of which irreversible polarization due to domain switching is accounted for. Numerical results computed with the plate model are compared to results using a three-dimensional formulation.

Key words: nonlinear plates, electro-elastic material surface, ferroelectric ceramics

1 CONSTITUTIVE RELATIONS

We start our discussion of the constitutive relations with relaxor ferroelectric ceramics by introducing a thermodynamic potential Ω per unit volume, the time derivative of which is

$$\dot{\Omega} = \boldsymbol{\sigma} \cdot\cdot \dot{\boldsymbol{\varepsilon}} - \boldsymbol{\mathcal{D}} \cdot \dot{\boldsymbol{\mathcal{E}}}, \tag{1}$$

see Eringen and Maugin [1]. Hence, we are discussing reversible constitutive processes at this point. $\boldsymbol{\varepsilon}$ is the strain tensor, $\boldsymbol{\sigma}$ the stress tensor, $\boldsymbol{\mathcal{E}}$ the electric field vector and $\boldsymbol{\mathcal{D}}$ the electric displacement vector. The thermodynamic potential is introduced as

$$\Omega(\boldsymbol{\varepsilon}, \boldsymbol{\mathcal{E}}) = \Phi(\boldsymbol{\varepsilon}, \boldsymbol{\mathcal{E}}) - \frac{1}{2}\varepsilon_0 \boldsymbol{\mathcal{E}} \cdot \boldsymbol{\mathcal{E}}. \tag{2}$$

Peer-review under responsibility of the organizing committee of SMART 2023.
doi: 10.7712/150123.9965.451024

Often, Ω is denoted as the augmented Helmholtz free energy, which is composed of the free energy Φ and an augmentation potential, in which ε_0 denotes the permittivity in vacuum. Then, the stress tensor $\boldsymbol{\sigma}$ and the electric displacement vector $\boldsymbol{\mathcal{D}}$ are derived from

$$\boldsymbol{\sigma} = \frac{\partial \Omega}{\partial \boldsymbol{\varepsilon}} \,, \quad \boldsymbol{\mathcal{D}} = -\frac{\partial \Omega}{\partial \boldsymbol{\mathcal{E}}}. \tag{3}$$

These constitutive relations are valid for elastic dielectrica in general, see Toupin [2]. Relaxor ferroelectric materials belong to this class of materials. Note, that our formulation does not account for ponderomotive forces. Next, the free energy is additively decomposed into an elastic part Φ_e and a dielectric part Φ_d; hence, $\Phi = \Phi_\mathrm{e} + \Phi_\mathrm{d}$. We introduce the elastic part as

$$\Phi_\mathrm{e}(\boldsymbol{\varepsilon}_\mathrm{e}) = \frac{1}{2} \boldsymbol{\varepsilon}_\mathrm{e} \cdot\cdot \mathbb{C} \cdot\cdot \boldsymbol{\varepsilon}_\mathrm{e}, \tag{4}$$

in which we have used the additive decomposition $\boldsymbol{\varepsilon} = \boldsymbol{\varepsilon}_e + \boldsymbol{\varepsilon}^*$ of the strain tensor into an elastic part $\boldsymbol{\varepsilon}_e$ and an electrostrictive eigenstrain $\boldsymbol{\varepsilon}^*$. $\mathbb{C}$ is the fourth rank elasticity tensor. In order to introduce the dielectric part, we start with the internal energy, in which we account for a linear and a nonlinear dielectric response

$$e_\mathrm{d} = \Psi(\boldsymbol{\mathcal{P}}_\mathrm{i}) + \frac{1}{2} (\boldsymbol{\mathcal{P}} - \boldsymbol{\mathcal{P}}_\mathrm{i}) \cdot (\varepsilon_0 \boldsymbol{\chi}_0)^{-1} \cdot (\boldsymbol{\mathcal{P}} - \boldsymbol{\mathcal{P}}_\mathrm{i}), \tag{5}$$

with the vacuum permittivity ε_0, the polarization $\boldsymbol{\mathcal{P}}$, a second rank susceptibility tensor $\boldsymbol{\chi}_0$ and an internal polarization $\boldsymbol{\mathcal{P}}_\mathrm{i}$. Applying the Legendre transformation $\Phi_\mathrm{d} = e_\mathrm{d} - \boldsymbol{\mathcal{E}} \cdot \boldsymbol{\mathcal{P}}$ the augmented free energy $\Omega = \Omega(\boldsymbol{\varepsilon}, \boldsymbol{\mathcal{E}}, \boldsymbol{\mathcal{P}}, \boldsymbol{\mathcal{P}}_\mathrm{i})$ takes the form

$$\Omega = \frac{1}{2} \boldsymbol{\varepsilon}_\mathrm{e} \cdot\cdot \mathbb{C} \cdot\cdot \boldsymbol{\varepsilon}_\mathrm{e} + \Psi(\boldsymbol{\mathcal{P}}_\mathrm{i}) + \frac{1}{2} (\boldsymbol{\mathcal{P}} - \boldsymbol{\mathcal{P}}_\mathrm{i}) \cdot (\varepsilon_0 \boldsymbol{\chi}_0)^{-1} \cdot (\boldsymbol{\mathcal{P}} - \boldsymbol{\mathcal{P}}_\mathrm{i}) - \boldsymbol{\mathcal{E}} \cdot \boldsymbol{\mathcal{P}} - \frac{1}{2} \varepsilon_0 \boldsymbol{\mathcal{E}} \cdot \boldsymbol{\mathcal{E}}. \tag{6}$$

In this formulation combining a linear with a nonlinear dielectric response, the augmented free energy depends on the strain tensor $\boldsymbol{\varepsilon}$, the electric field vector $\boldsymbol{\mathcal{E}}$, the polarization vector $\boldsymbol{\mathcal{P}}$ and the internal polarization $\boldsymbol{\mathcal{P}}_\mathrm{i}$. The eigenstrain accounts for electrostriction and it is therefore assumed as $\boldsymbol{\varepsilon}^* = \boldsymbol{\varepsilon}^*(\boldsymbol{\mathcal{P}})$. From the time derivative of the augmented free energy,

$$\dot{\Omega} = \frac{\partial \Omega}{\partial \boldsymbol{\varepsilon}} \cdot\cdot \dot{\boldsymbol{\varepsilon}} + \frac{\partial \Omega}{\partial \boldsymbol{\mathcal{E}}} \cdot \dot{\boldsymbol{\mathcal{E}}} + \frac{\partial \Omega}{\partial \boldsymbol{\mathcal{P}}} \cdot \dot{\boldsymbol{\mathcal{P}}} + \frac{\partial \Omega}{\partial \boldsymbol{\mathcal{P}}_\mathrm{i}} \cdot \dot{\boldsymbol{\mathcal{P}}}_\mathrm{i} = \boldsymbol{\sigma} \cdot\cdot \dot{\boldsymbol{\varepsilon}} - \boldsymbol{\mathcal{D}} \cdot \dot{\boldsymbol{\mathcal{E}}}, \tag{7}$$

we find the constitutive relations for $\boldsymbol{\sigma}$ and $\boldsymbol{\mathcal{D}}$ in the form of eq.(3). The derivatives of the augmented free energy with respect to $\boldsymbol{\mathcal{P}}$ and $\boldsymbol{\mathcal{P}}_\mathrm{i}$ vanish, because $\boldsymbol{\mathcal{P}}$ and $\boldsymbol{\mathcal{P}}_\mathrm{i}$ have the role of internal variables in the augmented free energy, such that their work conjugates must vanish. The resulting relations represent algebraic equations between the electric field, the polarization, the internal polarization and the stress. This formulation has been introduced in our previous work, see Pechstein et al. [3].

1.1 Isotropic relaxor ferroelectric ceramics

As a special case we consider isotropic relaxor ferroelectric ceramics with

$$\Omega = \mu\boldsymbol{\varepsilon}_e \cdot\cdot\, \boldsymbol{\varepsilon}_e + \frac{\lambda}{2}(\mathrm{tr}\boldsymbol{\varepsilon}_e)^2 + \Psi(\boldsymbol{\mathcal{P}}_\mathrm{i}) + \frac{1}{2}\frac{1}{\varepsilon_0\chi_0}(\boldsymbol{\mathcal{P}} - \boldsymbol{\mathcal{P}}_\mathrm{i})\cdot(\boldsymbol{\mathcal{P}} - \boldsymbol{\mathcal{P}}_\mathrm{i}) - \boldsymbol{\mathcal{E}}\cdot\boldsymbol{\mathcal{P}} - \frac{1}{2}\varepsilon_0\boldsymbol{\mathcal{E}}\cdot\boldsymbol{\mathcal{E}}, \quad (8)$$

with the Lame parameters μ and λ, and the susceptibility χ_0. We introduce the electrostrictive eigenstrain $\boldsymbol{\varepsilon}^* = \boldsymbol{\varepsilon}^*(\boldsymbol{\mathcal{P}})$ as

$$\boldsymbol{\varepsilon}^* = Q\left((1+\nu_\mathrm{Q})\boldsymbol{\mathcal{P}}\boldsymbol{\mathcal{P}} - \nu_\mathrm{Q}\mathbf{I}(\boldsymbol{\mathcal{P}}\cdot\boldsymbol{\mathcal{P}})\right), \quad (9)$$

with the electrostrictive coefficient Q and an electrostrictive Poisson ratio ν_Q. Finally, the potential $\Psi(\boldsymbol{\mathcal{P}}_\mathrm{i})$ must be specified. We chose it such that its derivative is

$$\frac{\partial\Psi}{\partial\boldsymbol{\mathcal{P}}_\mathrm{i}} = \frac{\mathcal{P}_\mathrm{sat}^m}{2\varepsilon_0\chi_\mathrm{i}(m-1)}\left((\mathcal{P}_\mathrm{sat} - \|\boldsymbol{\mathcal{P}}_\mathrm{i}\|)^{1-m} - (\mathcal{P}_\mathrm{sat} + \|\boldsymbol{\mathcal{P}}_\mathrm{i}\|)^{1-m}\right)\frac{\boldsymbol{\mathcal{P}}_\mathrm{i}}{\|\boldsymbol{\mathcal{P}}_\mathrm{i}\|}. \quad (10)$$

χ_i is a susceptibility, $\mathcal{P}_\mathrm{sat}$ the internal saturation polarization and m is a shape parameter. This family of potentials is also used for ferroelectric ceramics, see Pechstein et al. [4].

1.1.1 Plane stress

We assume a plane stress problem insofar as the stress tensor is taken as $\boldsymbol{\sigma} = \boldsymbol{\sigma}_2$. Here, $\boldsymbol{\sigma}_2$ refers to a plane perpendicular to $\boldsymbol{e}$ with $\boldsymbol{\mathcal{E}} = \mathcal{E}\boldsymbol{e}$, $\boldsymbol{\mathcal{P}} = \mathcal{P}\boldsymbol{e}$ and $\boldsymbol{\mathcal{P}}_\mathrm{i} = \mathcal{P}_\mathrm{i}\boldsymbol{e}$. Then, one can conclude that the strain tensor is $\boldsymbol{\varepsilon} = \boldsymbol{\varepsilon}_2 + \varepsilon_{33}\boldsymbol{e}\boldsymbol{e}$, in which $\boldsymbol{\varepsilon}_2$ refers to the plane part of $\boldsymbol{\varepsilon}$. Likewise, $\boldsymbol{\varepsilon}_\mathrm{e} = \boldsymbol{\varepsilon}_{\mathrm{e},2} + \varepsilon_{\mathrm{e},33}\boldsymbol{e}\boldsymbol{e}$ holds due to the specific form of $\boldsymbol{\varepsilon}^*$, which is

$$\boldsymbol{\varepsilon}^* = Q\left(\mathcal{P}^2\boldsymbol{e}\boldsymbol{e} - \nu_Q\mathcal{P}^2\mathbf{I}_2\right); \quad (11)$$

hence, we have $\boldsymbol{\varepsilon}_{\mathrm{e},2} = \boldsymbol{\varepsilon}_2 - \boldsymbol{\varepsilon}_2^*$ and $\varepsilon_{\mathrm{e},33} = \varepsilon_{33} - \varepsilon_{33}^*$ with $\boldsymbol{\varepsilon}_2^* = -\nu_Q Q\mathcal{P}^2\mathbf{I}_2$ and $\varepsilon_{33}^* = Q\mathcal{P}^2$. With these assumptions, we find the plane stress augmented free energy Ω_2 of an isotropic relaxor ferroelectric ceramic material to

$$\Omega_2 = \frac{1}{2}Y\left(\nu(\mathrm{tr}\boldsymbol{\varepsilon}_{\mathrm{e},2})^2 + (1-\nu)\boldsymbol{\varepsilon}_{\mathrm{e},2}\cdot\cdot\,\boldsymbol{\varepsilon}_{\mathrm{e},2}\right) + \Psi(\mathcal{P}_\mathrm{i}) + \frac{1}{2}\frac{1}{\varepsilon_0\chi_0}(\mathcal{P} - \mathcal{P}_\mathrm{i})^2 - \mathcal{E}\mathcal{P} - \frac{1}{2}\varepsilon_0\mathcal{E}^2. \quad (12)$$

$Y = \frac{E}{1-\nu^2}$ is the plane stress Young's modulus, with Young's modulus E and the Poisson ratio ν. Then, the plane stress constitutive relations and the derivatives of the plane stress augmented free energy with respect to $\mathcal{P}$ and $\mathcal{P}_\mathrm{i}$ are

$$\boldsymbol{\sigma}_2 = \frac{\partial\Omega_2}{\partial\boldsymbol{\varepsilon}_2}, \quad \mathcal{D} = -\frac{\partial\Omega_2}{\partial\mathcal{E}}, \quad \frac{\partial\Omega_2}{\partial\mathcal{P}} = 0, \quad \frac{\partial\Omega}{\partial\mathcal{P}_\mathrm{i}} = 0, \quad (13)$$

with the derivative of $\Psi(\mathcal{P}_\mathrm{i})$ as

$$\frac{\partial\Psi}{\partial\mathcal{P}_\mathrm{i}} = \frac{\mathcal{P}_\mathrm{sat}^m}{2\varepsilon_0\chi_\mathrm{i}(m-1)}\left((\mathcal{P}_\mathrm{sat} - |\mathcal{P}_\mathrm{i}|)^{1-m} - (\mathcal{P}_\mathrm{sat} + |\mathcal{P}_\mathrm{i}|)^{1-m}\right)\frac{\mathcal{P}_\mathrm{i}}{|\mathcal{P}_\mathrm{i}|}. \quad (14)$$

2 RELAXOR FERROELECTRIC PLATES

2.1 Plate augmented free energy

We assume a thin plate made of n layers; due to the thinness of the plate the plane stress assumption applies for each layer with a material behavior as introduced above. For the sake of simplicity only one layer is made of an isotropic relaxor ferroelectric material and the other layers are made of isotropic elastic materials. We introduce a reference surface with the thickness coordinate $Z = 0$. The i-th layer is located between $Z = Z_{i-1}$ and $Z = Z_i$. The single relaxor ferroelectric layer is assumed to be the k-th layer with thickness $h_\mathrm{f} = Z_k - Z_{k-1}$ and the center surface located at $Z_\mathrm{f} = 1/2(Z_k + Z_{k-1})$. Its top and bottom surface are electroded and an electric voltage V is applied. We start with the dielectric part of the plane stress augmented free energy from eq. (12), which is simply integrated through the thickness of the relaxor ferroelectric layer accounting for $\mathcal{E} = V h_\mathrm{f}^{-1}$; the result is

$$\omega_\mathrm{d} = \psi(\mathcal{P}_\mathrm{i}) + \frac{1}{2}\frac{1}{c_r}(\mathcal{P} - \mathcal{P}_\mathrm{i})^2 - V\mathcal{P} - \frac{1}{2}c_0 V^2 \tag{15}$$

ω_d is the dielectric part of the plate augmented free energy per unit area, $c_r = \varepsilon_0 \chi_0 h_\mathrm{f}^{-1}$, $c_i = \varepsilon_0 \chi_i h_\mathrm{f}^{-1}$ and $c_0 = \varepsilon_0 h_\mathrm{f}^{-1}$ are capacities per unit area. $\psi(\mathcal{P}_\mathrm{i})$ is obtained from eq. (14) by replacing $\varepsilon_0 \chi_i$ with c_i. For the elastic part of the plate augmented free energy we propose

$$\omega_\mathrm{e} = \frac{1}{2}A\left(\nu_A(\mathrm{tr}\mathbf{e}_\mathrm{e})^2 + (1-\nu_A)\mathbf{e}_\mathrm{e}\cdot\cdot\,\mathbf{e}_\mathrm{e}\right) + \frac{1}{2}D\left(\nu_D(\mathrm{tr}\boldsymbol{\kappa}_\mathrm{e})^2 + (1-\nu_D)\boldsymbol{\kappa}_\mathrm{e}\cdot\cdot\,\boldsymbol{\kappa}_\mathrm{e}\right). \tag{16}$$

Here, we have assumed the lamination scheme of the plate to be such that no coupling stiffness enters the formulation. A is the membrane stiffness, D the plate stiffness and ν_A and ν_D the corresponding plate Poisson ratios,

$$A = \sum_{i=1}^{n} Y_i h_i\,,\; A\nu_A = \sum_{i=1}^{n} Y_i \nu_i h_i\,,\; D = \sum_{i=1}^{n} \frac{Y_i(Z_i^3 - Z_{i-1}^3)}{3}\,,\; D\nu_D = \sum_{i=1}^{n} \frac{Y_i \nu_i (Z_i^3 - Z_{i-1}^3)}{3}. \tag{17}$$

$\mathbf{e}_\mathrm{e} = \mathbf{e} - \mathbf{e}^*$ is the elastic plate surface strain tensor, $\boldsymbol{\kappa}_\mathrm{e} = \boldsymbol{\kappa} - \boldsymbol{\kappa}^*$ the elastic plate curvature tensor, and $\mathbf{e}^* = e^*\mathbf{I}_2$ and $\boldsymbol{\kappa}^* = \kappa^*\mathbf{I}_2$ are the plate surface eigenstrain tensor and the plate eigencurvature tensor, which are defined as

$$e^* = \frac{1}{A(1+\nu_A)}\int_{Z_{k-1}}^{Z_k} Y_\mathrm{f}(1+\nu_\mathrm{f})\varepsilon_2^* dZ\,, \quad \kappa^* = \frac{1}{D(1+\nu_D)}\int_{Z_{k-1}}^{Z_k} Y_\mathrm{f}(1+\nu_\mathrm{f}) Z \varepsilon_2^* dZ, \tag{18}$$

with the plane part of the electrostrictive eigenstrain $\varepsilon_2^* = -\nu_Q Q \mathcal{P}^2$. Finally, $\mathbf{e}$ and $\boldsymbol{\kappa}$ are classical reference surface strain and curvature tensors of a plate, and the total plate augmented free energy per unit area is $\omega = \omega_\mathrm{e} + \omega_\mathrm{d}$.

2.2 Strain and curvature tensor of the plate

We consider thin plates as a two-dimensional generalized material surface, see [5], [6] and [7]. In particular, we consider the plate as a two-dimensional continuum with five mechanical degrees of freedom, three translations and two rotations, resembling the notion of a single rigid director $\boldsymbol{d}$ attached to each particle of the plate, see [8]. In case $\boldsymbol{d} \cdot \boldsymbol{d} = 1$ and $\boldsymbol{d} = \boldsymbol{n}$ with the unit normal vector of the material surface $\boldsymbol{n}$, we have a Kirchhoff-Love theory, see [9]. In an undeformed reference configuration the material surface is plane and denoted as reference surface. In a deformed actual configuration it is denoted as actual surface. The first and the second metric tensor of the reference surface are $\mathbf{A} = \mathbf{I}_2$ and $\mathbf{B} = \mathbf{0}$ with the two-dimensional identity tensor $\mathbf{I}_2 = \mathbf{I} - \boldsymbol{e}\boldsymbol{e}$; $\boldsymbol{e}$ is the constant unit normal vector of the reference surface. For the actual surface we have $\mathbf{a} = \nabla \boldsymbol{r} = \mathbf{I} - \boldsymbol{n}\boldsymbol{n}$ and $\mathbf{b} = \mathbf{b}^T = -\nabla \boldsymbol{n}$ with the differential operator ∇ of the actual surface, the position vector $\boldsymbol{r}$ in the deformed configuration and the unit normal vector $\boldsymbol{n}$ of the actual surface. The deformation gradient tensor of the material surface is $\mathbf{F} = (\nabla_0 \boldsymbol{r})^T$ with the differential operator $\nabla_0 = \mathbf{F}^T \cdot \nabla$ of the reference surface. We introduce the two tensor valued Green strain measures

$$\mathbf{e} = \frac{1}{2}\left(\mathbf{F}^T \cdot \mathbf{F} - \mathbf{I}_2\right) \ , \quad \boldsymbol{\kappa} = -\mathbf{F}^T \cdot \mathbf{b} \cdot \mathbf{F}, \tag{19}$$

which remain constant if and only if the motion of the material surface is a rigid body motion, see [10] for details. These strain measure resemble the surface strain tensor and the curvature tensor used in our formulation.

2.3 Thermodynamics and constitutive relations

In the case of a plate theory for relaxor ferroelectric plates, the counterpart to eq.(1) is

$$\boldsymbol{\tau} \cdot\cdot\, \dot{\mathbf{e}} + \boldsymbol{\mu} \cdot\cdot\, \dot{\boldsymbol{\kappa}} - \mathcal{D}\dot{V} - \dot{\omega} = 0. \tag{20}$$

With $\omega = \omega(\mathbf{e}, \boldsymbol{\kappa}, V, \mathcal{P}, \mathcal{P}_\mathrm{i})$ we find

$$\left(\boldsymbol{\tau} - \frac{\partial \omega}{\partial \mathbf{e}}\right) \cdot\cdot\, \dot{\mathbf{e}} + \left(\boldsymbol{\mu} - \frac{\partial \omega}{\partial \boldsymbol{\kappa}}\right) \cdot\cdot\, \dot{\boldsymbol{\kappa}} - \left(\mathcal{D} + \frac{\partial \omega}{\partial V}\right) \dot{V} - \frac{\partial \omega}{\partial \mathcal{P}} \dot{\mathcal{P}} - \frac{\partial \omega}{\partial \mathcal{P}_\mathrm{i}} \dot{\mathcal{P}}_\mathrm{i} = 0, \tag{21}$$

from which the constitutive relations of the plate follow to

$$\boldsymbol{\tau} = \frac{\partial \omega}{\partial \mathbf{e}} \ , \quad \boldsymbol{\mu} = \frac{\partial \omega}{\partial \boldsymbol{\kappa}} \ , \quad \mathcal{D} = -\frac{\partial \omega}{\partial V} \ , \quad 0 = \frac{\partial \omega}{\partial \mathcal{P}} \ , \quad 0 = \frac{\partial \omega}{\partial \mathcal{P}_i}. \tag{22}$$

3 EXTENSION TO FERROELECTRIC PLATES

Now, we proceed to extending the plate formulation to irreversible constitutive processes. In particular, we study plates made of ferroelectric materials, rather than relaxor ferroelectric materials. The extension is straightforward. First, we note, that the internal polarization used for relaxor ferroelectrics translates to the irreversible polarization for ferroelectric materials,

by means of which irreversible domain switching is accounted for. Then, the Clausius-Duhem inequality in the form

$$\boldsymbol{\tau} \cdot\cdot \dot{\mathbf{e}} + \boldsymbol{\mu} \cdot\cdot \dot{\boldsymbol{\kappa}} - \mathcal{D}\dot{V} - \dot{\omega} \geq 0 \tag{23}$$

is used as a starting point for this extension. With the plate augmented free energy $\omega = \omega(\mathbf{e}, \boldsymbol{\kappa}, V, \mathcal{P}, \mathcal{P}_\mathrm{i})$ the Clausius-Duhem inequality reads

$$\left(\boldsymbol{\tau} - \frac{\partial \omega}{\partial \mathbf{e}}\right) \cdot\cdot \dot{\mathbf{e}} + \left(\boldsymbol{\mu} - \frac{\partial \omega}{\partial \boldsymbol{\kappa}}\right) \cdot\cdot \dot{\boldsymbol{\kappa}} - \left(\mathcal{D} + \frac{\partial \omega}{\partial V}\right) \dot{V} - \frac{\partial \omega}{\partial \mathcal{P}} \dot{\mathcal{P}} - \frac{\partial \omega}{\partial \mathcal{P}_\mathrm{i}} \dot{\mathcal{P}}_\mathrm{i} \geq 0. \tag{24}$$

Recalling the constitutive relations for reversible relaxor ferroelectric ceramics and the fact that the present irreversible constitutive process of domain switching is accounted for by means of $\mathcal{P}_\mathrm{i}$, we conclude that the first four terms in the Clausius-Duhem inequality must vanish, and a reduced dissipation inequality follows to $\mathcal{F}_\mathrm{i}\dot{\mathcal{P}}_\mathrm{i} \geq 0$. $\mathcal{F}_\mathrm{i}$ is the so-called "driving force"

$$\mathcal{F}_\mathrm{i} = -\frac{\partial \omega}{\partial \mathcal{P}_\mathrm{i}}, \tag{25}$$

by means of which the irreversible process is driven. For relaxor ferroelectric ceramic plates $\mathcal{F}_\mathrm{i} = 0$ holds. Finally, we introduce a switching criterion, which limits the magnitude of the "driving force"; hence,

$$\phi(\mathcal{F}_\mathrm{i}) = |\mathcal{F}_\mathrm{i}| - V_c \leq 0, \tag{26}$$

with a coercive voltage V_c. We apply the principle of maximum dissipation, see [11] for rate-independant plasticity, to satisfy the reduced dissipation inequality accounting for the inequality constraint $|\mathcal{F}_\mathrm{i}| - V_c \leq 0$ in the corresponding optimization problem, the solution of which are the Karush-Kuhn-Tucker (KKT) conditions

$$\phi \leq 0\,, \quad \lambda \geq 0\,, \quad \lambda\phi = 0 \quad \text{and} \quad \dot{\mathcal{P}}_\mathrm{i} = \lambda \frac{\partial \phi}{\partial \mathcal{F}_\mathrm{i}} = \lambda \mathrm{sgn}(\mathcal{F}_\mathrm{i}), \tag{27}$$

where λ is a Lagrange multiplier. Alternatively, we satisfy the principle of maximum dissipation by introducing a so-called dissipation function $\varphi(\dot{\mathcal{P}}_\mathrm{i})$ as suggested by Miehe et al. [12],

$$\varphi(\dot{\mathcal{P}}_\mathrm{i}) = V_c|\dot{\mathcal{P}}_\mathrm{i}| = \sup_{|\mathcal{F}_\mathrm{i}| \leq V_c} (\mathcal{F}_\mathrm{i}\dot{\mathcal{P}}_\mathrm{i}), \tag{28}$$

which can be shown to be equal to the maximum dissipation. We note two more important characteristics of the dissipation function,

$$\frac{\partial \varphi}{\partial \dot{\mathcal{P}}_\mathrm{i}} \dot{\mathcal{P}}_\mathrm{i} = \varphi \quad \text{and} \quad \mathcal{F}_\mathrm{i} = \frac{\partial \varphi}{\partial \dot{\mathcal{P}}_\mathrm{i}} \text{ for } \lambda > 0. \tag{29}$$

In contrast to relaxor ferroelectric ceramics, ferroelectric ceramics exhibit a piezoelectric effect; this must be accounted for as well. In order to do so, we extend the plane part of the eigenstrain tensor $\boldsymbol{\varepsilon}_2^*$ according to

$$\boldsymbol{\varepsilon}_2^* = \left(\frac{\mathcal{P}_\mathrm{i}}{\mathcal{P}_\mathrm{sat}} d\mathcal{E} - \nu_Q Q \mathcal{P}^2\right) \mathbf{I}_2 = \varepsilon_2^* \mathbf{I}_2, \tag{30}$$

in which $d = d_{31}$ is a nominal piezoelectric coefficient.

3.1 Generalized principle of virtual work

We introduce a generalized principle of virtual work for ferroelectric plates

$$0 = \delta A^{(\mathrm{e,b})} + \int_{A_0} (\boldsymbol{p} \cdot \delta \boldsymbol{r} + \boldsymbol{m} \times \boldsymbol{n} \cdot \delta \boldsymbol{n} - \sigma \delta V)\, dA_0 + \int_{A_0} \delta a^{(\mathrm{i})} dA_0, \tag{31}$$

which was used before for piezoelectric plates and shells by [5] and for dielectric elastomer plates by [6] and [7]. $\boldsymbol{p}$, $\boldsymbol{m}$ and σ are external mechanical forces and moments and electrical charges per unit area of the reference surface with area A_0. External forces and moments acting at the boundary are accounted for by means of the virtual work $\delta A^{(\mathrm{e,b})}$. $\delta a^{(\mathrm{i})}$ is the virtual work of the internal forces and moments and of the internal electrical charges,

$$\delta a^{(i)} = -\boldsymbol{\tau} \cdot\cdot\, \delta \mathbf{e} - \boldsymbol{\mu} \cdot\cdot\, \delta \boldsymbol{\kappa} + \mathcal{D} \delta V. \tag{32}$$

From the variation of the plate augmented free energy $\omega = \omega(\mathbf{e}, \boldsymbol{\kappa}, V, \mathcal{P}, \mathcal{P}_\mathrm{i})$ and taking into account the constitutive relations of ferroelectric plates we obtain

$$\delta \omega = \boldsymbol{\tau} \cdot\cdot\, \delta \mathbf{e} + \boldsymbol{\mu} \cdot\cdot\, \delta \boldsymbol{\kappa} - \mathcal{D} \delta V + \frac{\partial \omega}{\partial \mathcal{P}_\mathrm{i}} \delta \mathcal{P}_\mathrm{i} = -\delta a^{(i)} - \mathcal{F}_\mathrm{i} \delta \mathcal{P}_\mathrm{i}, \tag{33}$$

such that the principle of virtual work is

$$\delta(W + \Omega) + \int_{A_0} \frac{\partial \varphi}{\partial \dot{\mathcal{P}}_\mathrm{i}} \delta \mathcal{P}_\mathrm{i} = 0 \quad \text{with } W = \int_{A_0} w dA_0\ , \quad \Omega = \int_{A_0} \omega dA_0. \tag{34}$$

Here, we have assumed all external loadings to be conservative with the specific potential energy w of the external loadings. From eq.(34) we derive an incremental stationarity principle. With $\Omega_{n+1} = \Omega_n + \Delta\Omega_n$, $W_{n+1} = W_n + \Delta W_n$ and $\mathcal{P}_{\mathrm{i},n+1} = \mathcal{P}_{\mathrm{i},n} + \Delta\mathcal{P}_{\mathrm{i},n}$, we have

$$\delta(\Delta W_n + \Delta\Omega_n) + \int_{A_0} \frac{\partial \varphi}{\partial \dot{\mathcal{P}}_\mathrm{i}} \delta(\Delta \mathcal{P}_{\mathrm{i},n}) dA_0 = 0, \tag{35}$$

in which we approximate $\frac{\partial \varphi}{\partial \dot{\mathcal{P}}_\mathrm{i}}$, such that

$$\frac{\partial \varphi}{\partial \dot{\mathcal{P}}_\mathrm{i}} \delta(\Delta \mathcal{P}_{\mathrm{i},n}) = V_c \frac{\dot{\mathcal{P}}_\mathrm{i}}{|\dot{\mathcal{P}}_\mathrm{i}|} \delta(\Delta \mathcal{P}_{\mathrm{i},n}) \approx V_c \frac{\Delta \mathcal{P}_{\mathrm{i},n}}{|\Delta \mathcal{P}_{\mathrm{i},n}|} \delta(\Delta \mathcal{P}_{\mathrm{i},n}) = \delta\left(V_c |\Delta \mathcal{P}_{\mathrm{i},n}|\right) \tag{36}$$

holds. The final form of the incremental stationarity principle

$$\delta \left(\Delta W_n + \Delta\Omega_n + \int_{A_0} V_c |\Delta \mathcal{P}_{\mathrm{i},n}| dA_0 \right) = 0, \tag{37}$$

is the starting point for numerical solutions using the finite element method. Relaxor ferroelectric ceramic plates are included with $V_c = 0$ and $d = 0$.

4 EXAMPLES

In this section, we present numerical results for bi-morph plates made of either relaxor ferroelectric ceramics or of ferroelectric ceramics. The top layer is electroded at both horizontal surfaces and actuated by a voltage V; no other loadings are considered. The bottom layer is assumed to be purely elastic with the elasticity parameters taken as the one of the top layer. The dimensions are $a \times b \times h = 4\text{mm} \times 2\text{mm} \times 0.02\text{mm}$, in which h is the total thickness of the bi-morph plate; hence, $h_\text{f} = h/2$. The bi-morph plate is either clamped at $x = 0$, see fig. 1, or it is clamped at $x = 0$ and at $x = a$; the latter case is not shown.

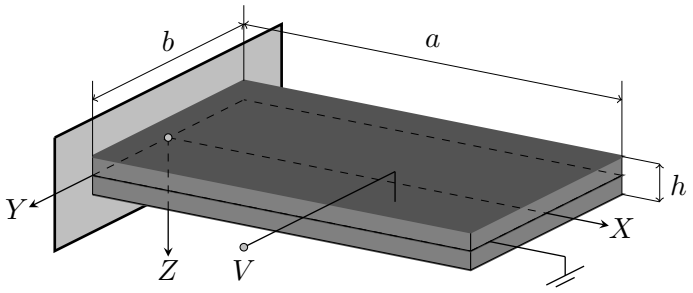

Figure 1: Sketch of the bi-morph plate (dimensions $a \times b \times h$) clamped at $x = 0$; electric potential V is applied at the top electrode of the top layer and the center electrode is grounded.

The plate augmented free energy is

$$\begin{aligned}\omega = &\frac{1}{2}A\left(\nu_A(\text{tr}\mathbf{e}_\text{e})^2 + (1-\nu_A)\mathbf{e}_\text{e}\cdot\cdot\,\mathbf{e}_\text{e}\right) + \frac{1}{2}D\left(\nu_D(\text{tr}\boldsymbol{\kappa}_\text{e})^2 + (1-\nu_D)\boldsymbol{\kappa}_\text{e}\cdot\cdot\,\boldsymbol{\kappa}_\text{e}\right)\\ &+ \psi(\mathcal{P}_\text{i}) + \frac{1}{2}\frac{1}{c_r}(\mathcal{P}-\mathcal{P}_\text{i})^2 - V\mathcal{P} - \frac{1}{2}c_0V^2;\end{aligned} \tag{38}$$

$\psi(\mathcal{P}_\text{i})$ is defined by eq. (14). The capacities per unit area in the energy are $c_r = 2\varepsilon_0\chi_0/h$, $c_0 = 2\varepsilon_0/h$, $c_i = 2\varepsilon_0\chi_i/h$ and stiffnesses and Poisson ratios are

$$A = \frac{Eh}{1-\nu^2}\,, \quad D = \frac{Eh^3}{12(1-\nu^2)}\,, \quad \nu_A = \nu_D = \nu. \tag{39}$$

The eigenstrain $\boldsymbol{\varepsilon}^* = \varepsilon^*\mathbf{I}_2$ and the eigencurvature $\boldsymbol{\kappa}^* = \kappa^*\mathbf{I}_2$ are computed from

$$\varepsilon^* = \frac{E_2^*}{2}\,,\ \kappa^* = -\frac{3E_2^*}{2h} \quad \text{with} \quad E_2^* = \frac{\mathcal{P}_i}{\mathcal{P}_\text{sat}}d\frac{2V}{h} - \nu_Q Q\mathcal{P}^2. \tag{40}$$

Numerical results are computed with the Finite Element method. We use an extension of mixed shell elements, which were developed by Neunteufel and Schöberl [15] for elastic shells. For details of these electro-mechanically coupled shell elements we refer to another contribution to the present proceedings, see Pechstein et al. [16].

4.1 Relaxor ferroelectric ceramic bi-morph plate made of PNM-PT-BT

We use a PMN-PT-BT relaxor ferroelectric material at 5°C with material parameters taken from Hom and Shankar [13], which are shown in tab. 1. These material parameters are related to the ones used in our formulation by means of $Q = Q_{111}$, $Q\nu_Q = -Q_{122}$ and $\varepsilon_0\chi_\mathrm{i} = \mathcal{P}_\mathrm{sat}k$. For the Poisson ratio we have chosen $\nu = 0.4$, as it has not been given in the original reference [13]. Also note that $\chi_0 = 0$ in [13], such that $\mathcal{P}_\mathrm{i} = \mathcal{P}$ in our formulation, and the bi-morph plate

E/Nm^2	$Q_{111}/\mathrm{m}^4\mathrm{C}^{-2}$	$Q_{122}/\mathrm{m}^4\mathrm{C}^{-2}$	$\mathcal{P}_\mathrm{sat}/\mathrm{Cm}^{-2}$	k/mV^{-1}
97×10^9	13.3×10^{-3}	-6.06×10^{-3}	0.259	1.16×10^{-6}

Table 1: Material parameters for a PMN-PT-BT relaxor ferroelectric at 5°C taken from [13].

augmented energy reduces to

$$\omega(\boldsymbol{\varepsilon}, \boldsymbol{\kappa}, \mathcal{P}, V) = \frac{1}{2}A\left(\nu(\mathrm{tr}\mathbf{e}_\mathrm{e})^2 + (1-\nu)\mathbf{e}_\mathrm{e}\cdot\cdot\,\mathbf{e}_\mathrm{e}\right) + \frac{1}{2}D\left(\nu(\mathrm{tr}\boldsymbol{\kappa}_\mathrm{e})^2 + (1-\nu)\boldsymbol{\kappa}_\mathrm{e}\cdot\cdot\,\boldsymbol{\kappa}_\mathrm{e}\right) + \psi(\mathcal{P}) - V\mathcal{P} - \frac{1}{2}c_0V^2, \tag{41}$$

in which $\mathcal{P}$ replaces $\mathcal{P}_\mathrm{i}$ in $\psi(\mathcal{P}_\mathrm{i})$ and $E_2^* = -\nu_Q Q\mathcal{P}^2$; for the shape parameter we use $m = 1$. We study the bi-morph plate clamped at $x = 0$. The applied voltage V is increased up to $V = 40\mathrm{V}$. The end point deflection at $X = a$ and $Y = 0$ is presented in fig. 2. The applied voltage in the

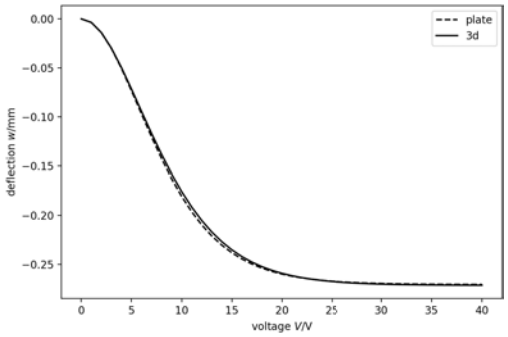

Figure 2: End point deflection vs. voltage V

top layer results in a negative in-plane eigenstrain, which is why the plate bends upwards. After a quadratic increase as a function of the applied voltage, the deflection saturates. This can be explained, because the polarization saturates to the saturation polarization $\mathcal{P}_\mathrm{sat}$ as the voltage increases; hence, the resulting electrostrictive actuation saturates as well. In the plot we have included results computed within a 3D theory developed by the authors, see Pechstein et al. [3]. Clearly results computed with the present plate formulation deviate only slightly from the full 3D results.

4.2 Ferroelectric ceramic bi-morph plate made of PZT-5H

Next we study the ferroelectric behavior of the bi-morph made of PZT-5H with material parameters taken from Pechstein et al. [14], which are given in tab. 2. These material parameters are

E/Nm^2	$\nu/1$	$\varepsilon_T/\mathrm{CV}^{-1}\mathrm{m}^{-1}$	d_{31}/mV^{-1}
61×10^9	0.31	2.77×10^{-8}	-2.74×10^{-10}
e_c/Vm^{-1}	$\mathcal{P}_{\mathrm{sat}}/\mathrm{Cm}{-}2$	$S_{\mathrm{sat}}/1$	h_0/VmC^{-1}
820×10^3	0.24	9.3×10^{-3}	714×10^3

Table 2: Material parameters for a PZT-5H taken from [14].

related to the ones in our formulation by means of $Q = S_{\mathrm{sat}}/\mathcal{P}_{\mathrm{sat}}^2$, $\varepsilon_0\chi_0 = \varepsilon_T$, $\varepsilon_0\chi_i = h_0^{-1}$, $V_c = e_c h/2$; also $\nu_Q = 0.5$ and $m = 1$ are used. Note, that we assume the electrostrictive part of the plane stress eigenstrain to depend on $\mathcal{P}_{\mathrm{i}}$ rather than on $\mathcal{P}$,

$$E_2^* = \frac{\mathcal{P}_{\mathrm{i}}}{\mathcal{P}_{\mathrm{sat}}} d\mathcal{E} - \nu_Q Q \mathcal{P}_{\mathrm{i}}^2. \tag{42}$$

We study the bi-morph plate either clamped only at $X = 0$ or clamped at $X = 0$ and $X = a$. A cyclic voltage is applied to the top layer with $V = \pm 40\mathrm{V}$. The resulting hystereses for the

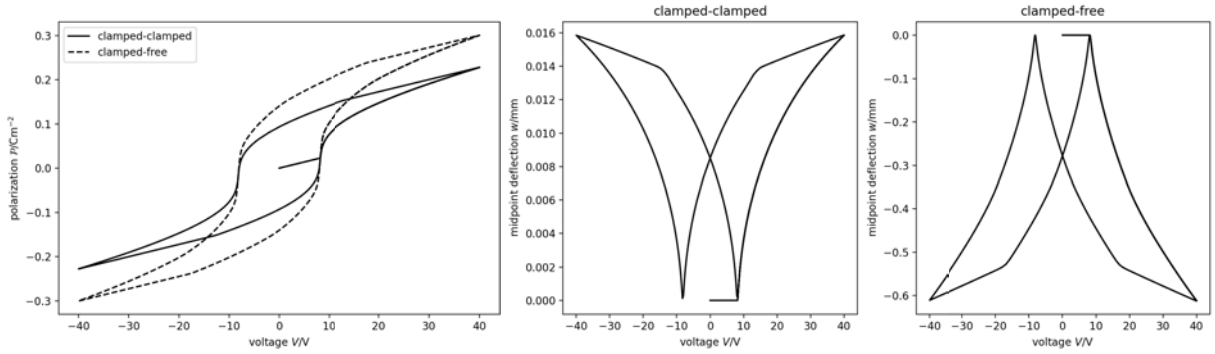

Figure 3: Ferroelctric hystereses (left) and butterfly hystereses (center & right) vs. voltage V

polarization are shown in the left plot in fig. 3 and the ones for the deflection in the center and the right plot. Polarization and deflection are presented for $X = a/2$ and $Y = 0$. From the polarization plot we see, that up to $V = V_c = 8.2\mathrm{V}$ no irreversible polarization occurs and we have a linear behavior; above the coercive voltage $\mathcal{P}_{\mathrm{i}}$ evolves until it starts to saturate. Proceeding further, the ferroelectric hystereses are obtained. The corresponding butterfly hystereses for the deflection are shown in the center and right plot. Clearly, the deflection is much smaller in the clamped-clamped case as deformations are strongly constrained, see also fig. 4 for deformed configurations. Hence, tensile stresses perpendicular to the direction of the irreversible polarization occur, which hinders the evolution of the irreversible polarization. In contrast, the

clamped-free plate is nearly stress free, such that $\mathcal{P}_\mathrm{i}$ can evolve freely. This also explains, why the polarization is smaller in the clamped-clamped case.

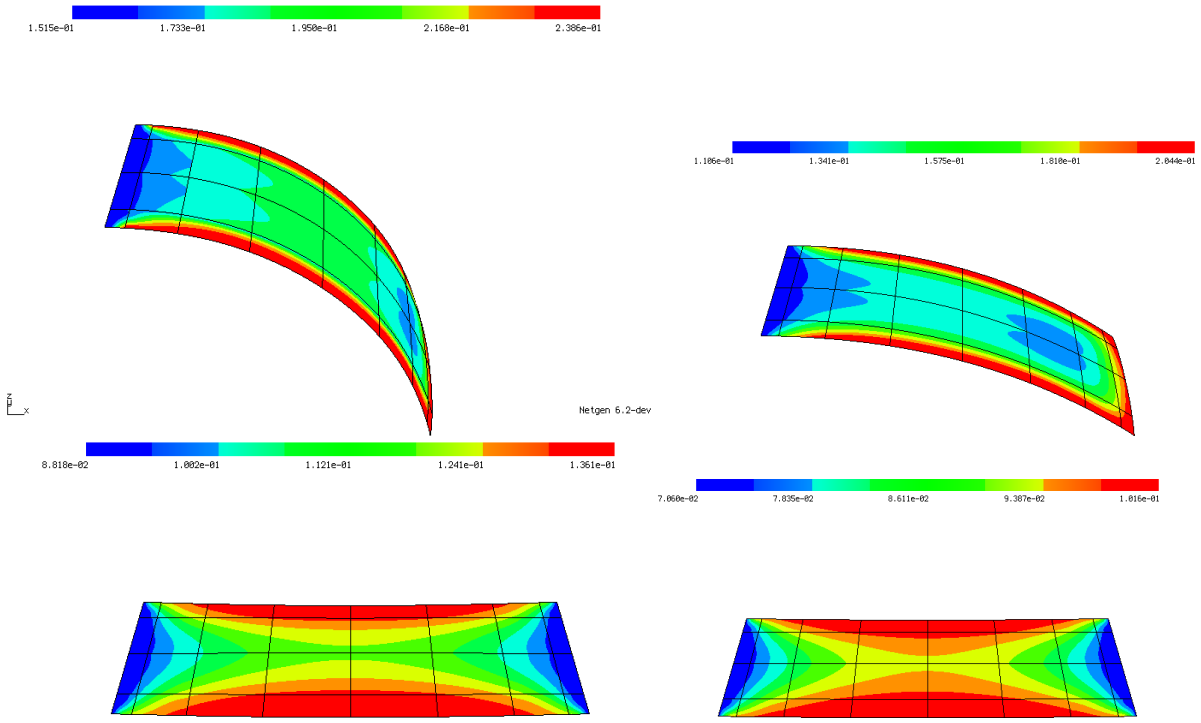

Figure 4: Irreversible polarization as contour plot in the deformed configuration for clamped-free plate (top) and clamped-clamped plate (bottom) after loading with $V = 40\mathrm{V}$ (left) and unloading with $V = 0\mathrm{V}$ (right).

A comparison of the results for ferroelectric ceramic plates with 3D computations is left for future work. Extensions of the present formulation to the case of ferroelectric polymers are ongoing; for first results see the contribution by Pechstein et al. [16] to the present proceedings.

REFERENCES

[1] Eringen AC and Maugin GA (1990) *Electrodynamics of Continua I: Foundations and Solid Media*. Springer New York, NY.

[2] Toupin RA (1956) The Elastic Dielectric. *Journal of Rational Mechanics and Analysis* 5(6): 849–915.

[3] Pechstein AS, Krommer M and Humer A (2022) Modeling and numerical simulation of electrostrictive materials and structures. *Smart Structures and Systems* 30(3): 221–237.

[4] Pechstein AS, Meindlhumer M and Humer A (2021) High-order mixed finite elements for

an energy-based model of the polarization process in ferroelectric materials. *Journal of Intelligent Material Systems and Structures* 32(3): 355–368.

[5] Vetyukov Yu, Staudigl E and Krommer M (2018) Hybrid asymptotic-direct approach to finite deformations of electromechanically coupled piezoelectric shells. *Acta Mechanica* 229(2): 953–974.

[6] Hansy-Staudigl E, Krommer M and Vetyukov Yu (2018) Finite deformations of thin plates made of dielectric elastomers: Modeling, Numerics and Stability. *Journal of Intelligent Material Systems and Structures* 29(17): 3495–3513.

[7] Hansy-Staudigl E, Krommer M and Humer A (2019) A complete direct approach to nonlinear modeling of dielectric elastomer plates. *Acta Mechanica* 230: 3923–3943.

[8] Naghdi P (1972) The theory of shells and plates. In *Handbuch der Physik* **VIa/2**, Flügge S and Truesdell C (eds.) 425–640, Springer, Berlin.

[9] Altenbach H and Eremeyev VA (2013) Cosserat-Type Shells. In *Generalized Continua from the Theory to Engineering Applications*, Altenbach H and Eremeyev VA (eds.), CISM International Centre for Mechanical Sciences (Courses and Lectures) 541, Springer, Vienna.

[10] Vetyukov Y (2014) *Nonlinear Mechanics of Thin-Walled Structures: Asymptotics, Direct Approach and Numerical Analysis*, SpringerViennaNewYork.

[11] Simo JC and Hughes TJR (1998) *Computational Inelasticity*, Springer, New York.

[12] Miehe C., Rosato D and Kiefer B (2011) Variational principles in dissipative electro-magneto-mechanics: a framework for the macro-modeling of functional materials. *International Journal for Numerical Methods in Engineering* 86(10): 1225–1276.

[13] Hom CL and Shankar N (1994) A Fully Coupled Constitutive Model for Electrostrictive Ceramic Materials. *Journal of Intelligent Material Systems and Structures* 5: 795–801.

[14] Pechstein A, Meindlhumer M, Humer A and Krommer M (2022) Locking Free High-Order Mixed Elements for Ferroeletric Polarization. In *Dynamics and Control of Advanced Structures and Machines*, Irschik H, Krommer M, Matveenko VP and Belyaev AK (eds.), Advanced Structured Materials 156: 173–185, Springer, Cham.

[15] Neunteufel M and Schöberl J (2019) The hellan–herrmann–johnson method for nonlinear shells. *Computers & Structures* 225: 106109.

[16] Pechstein A, Krommer M and Vetyukov Y (2023) Efficient Simulation of Electromechanical Coupling Effects in Thin Shells at Large Deformations. In *Proc. of X ECCOMAS Thematic Conference on Smart Structures and Materials (SMART 2023)*, Saravanos DA, Benjeddou A, Chrysochoidis N and Theodosiou T (eds.).